Comparison of pore-size distribution of soils obtained by different methods

Min Wang
Zienkiewicz Centre for Computational Engineering, College of Engineering, Swansea University, Singleton Park, Swansea, SA2 8PP, UK
Email: sacewangmin@gmail.com

G.N. Pande
Zienkiewicz Centre for Computational Engineering, College of Engineering, Swansea University, Singleton Park, Swansea, SA2 8PP, UK
Email: g.n.pande@swansea.ac.uk

L.W. Kong
State Key Laboratory of Geomechanics and Geotechnical Engineering, Institute of Rock and Soil Mechanics, Chinese Academy of Sciences, Wuhan, 430071, China
Email: lwkong@whrsm.ac.cn

Y.T. Feng
Zienkiewicz Centre for Computational Engineering, College of Engineering, Swansea University, Singleton Park, Swansea, SA2 8PP, UK
Email: y.feng@swansea.ac.uk

Abstract

An average size of pores and pore-size distribution (POSD) is often required for advanced constitutive models for soils adopted for hydro-mechanical-thermal coupled problems. There are a number of methods available for determining POSD, most requiring specific testing equipment and expertise. In this technical note a comparison is made of POSDs obtained from two different techniques viz, Mercury Intrusion Porosimetry (MIP) and the Pressure Plate Test (PPT). The former requires a specialists' apparatus not commonly available in Soils Laboratories and also has safety issues whilst the latter is more common as it is used to determine Soil Water Retention Characteristics of soils. On the basis of certain assumptions, it is demonstrated that POSDs obtained from the two techniques, match well and PPT can be used by researchers in soil mechanics to obtain POSD. The range of pore sizes determined by the two techniques is, however, different. Besides, the POSD obtained from other Soil Water Retention Curve (SWRC) techniques are compared with MIP data. A better correlation between POSD and SWRC can be observed.

Keywords

Soil Water Retention Curve, Pressure plate test; Mercury intrusion; Pore-size and Particle-size distributions; Gradation curve of soils

Introduction

Soil mass is a collection of soil particles of various sizes and shapes with pores filled with air and water. Pore Size Distribution (POSD) is critical in understanding its physical, mechanical and hydraulic behaviour of soils. POSD affects their permeability (Dullien, 1991, Bryant and Blunt, 1992, Shin et al., 2015), deformation characteristics (Pietruszczak and Pande, 1991, Pietruszczak and Pande, 1996), as well as thermal conductivity (Gibson and Ashby, 1999). Therefore, measurement of POSD of porous media has been a topic of research for many decades. Several techniques have been developed and they are briefly described below:

1) Mercury Intrusion Porosimetry (MIP) is a well-known technique which is used to determine POSD for porous media like rock, concrete, building materials etc. Here, mercury at increasingly higher pressures is injected into the porous material and volume injected is recorded. The MIP technique allows the analysis of POSD over the range of approximately 0.0036μm to 1000μm. However, at high pressures, breaking the particles and opening closed pores (Penumadu and Dean, 2000, Kuila and Prasad, 2013) may significantly affect the accuracy of the size of small pores. Despite these limitations, the ability of MIP to record pores (>50 nm) makes it a very useful tool (Drake, 1949, Diamond, 1970, Delage, 2007, Romero and Simms, 2008).

2) Another technique is that of Nitrogen Adsorption (NA) (Echeverría et al., 1999, Kuila and Prasad, 2013). Here, a degassed sample is exposed to nitrogen gas at constant temperature (−197.3℃) at a series of precisely controlled pressures. Gas in pores with different diameters will condense at different pressures and this can obtain the distribution of pore sizes of the sample. In NA technique, the effective pore size ranges from 1 nm to 400 nm.

3) POSD can also be determined by Image Analysis methods including the 2D Scanning Electrone Microscopy (SEM) (Doktor et al., 2010) and 3D X-ray Computer Tomography (Lindquist et al., 2000, Shin et al., 2013). As the 2D SEM has limitation in the characterisation of pore structures, the CT technique has been utilised for the measurement POSD in recent years.

It is noted that POSD can also be estimated by correlating it to Particle Size Distribution (PSD) by assuming shape of particles as spherical or oval (Arya and Paris, 1981, Arya et al., 1999). Imre et al. (2012) used 'transfer functions' to obtain POSD from grading curves of sandy soils.

It is well known that all methods are approximate, have limited range of applicability and are based on certain assumptions. They require special equipment and expertise which is not generally available in Soils laboratories. All techniques except PSD have safety issues as well.

In this paper results of POSD of a soil obtained from the Pressure Plate Test (PPT) facility (Richards, 1941), commonly available in the laboratory of soil science, are compared with those from MIP tests on the same soil. In the next section a brief description of PPT is given for clarity and completeness. Next, POSD of a soil is obtained from PPT as well as from MIP. The correlation between the two is seen to be excellent. Experimental data reported by other researchers also indicate the same trend. Conclusions and recommendations for future research are given at the end.

Pressure plate test

Equipment:

The pressure plate equipment used in this study is made by the American Soil Moisture Equipment Corporation. It essentially consists of a pressure vessel which can be pressurised by nitrogen up to a pressure of 1500 kPa. A number of saturated soil samples 61.8 mm in diameter and 20.0 mm in thickness are placed on a ceramic disc which has a specified air entry pressure value. The disc is connected to the atmosphere and water is allowed to flow out freely. Nitrogen pressure is applied in steps with pressure being held at some fixed values viz.10, 30, 50, 100, 300, 500, 1200 kPa, During the whole test, the temperature in the laboratory was controlled around 20℃. The change in moisture content of the sample is determined by weighing it using electronic scales having accuracy of +/-0.01g every 12 hours for every pressure step. If the mass of the sample remains unchanged after 24 hours, it is assumed to be in equilibrium. A typical graph between water content and time is shown in Fig. 1. A graph between suction which is equal to applied nitrogen pressure, water pressure being zero, is plotted against moisture content or degree of saturation.

The Soil:

The soil tested in this study was taken from 1.8-2.5 meters below the surface of a slope at the Institute of Buffalo, Academy of Agriculture, in the suburb of Nanning, Guangxi Province, China. Table 1 indicates the basic physical properties of the soil. The gradation curve of this soil is given in Fig. 2.

Experimental results and discussions

Fig. 3 shows the Soil Water Retention Curve (SWRC) in which water content expressed as percent is plotted against logarithm coordinate of suction pressures. This represents the drying or desiccation process where a fully saturation sample has a decreasing water content. The sample can be wetted again and it is known that the wetting curve will produce a hysteretic loop. However this is not relevant to the theme of this paper. To determine the pore-size distribution from the SWRC, the following three assumptions are made:

1) As suction is progressively increased, water in the larger pores is progressively replaced by air. This in turn leads to a microstructure of desaturation which is schematically shown in Fig. 4. Here a pore-tube (a channel formed by connecting pores of the same size) of the largest diameter gets emptied first followed by successively smaller diameter tubes.

2) It is assumed that the volume of water adheres or is chemically bonded to the grains can be neglected compared to pore water. This is a first approximation and it may be possible to establish a 'residual' water content or 'residual' degree of saturation. If this can be accounted for, a correction can be applied to pore-size distribution. However the procedure as described here will still be valid.

3) The effect of nitrogen getting dissolved in pore water is ignored. It is obviously possible to apply a 'correction' to account for this.

Adopting the above assumptions, PPTs can be treated as gas intrusion tests (where gas is the non-wetting fluid) similar to mercury expel gas in MIP tests. As in MIP test, the non-wetting fluid, air, cannot intrude pores in PPT unless a pressure higher than the water pressure in pores is applied. Thus, different suction pressures correspond to penetration of air in different pore sizes which can be determined using the Washburn equation.

$$d = \left(4T_s cos\alpha\right)/P \qquad (1)$$

where d is the soil pore diameter, T_s is the surface tension, α is the contact angle between the soil particles and the fluid, P is the applied pressure or the capillary/suction pressure.

The influence factors of surface tension mainly include temperature, liquid type and the contact interface between different fluids, e.g. gas and water; While, the contact angle can be affected by physical properties of solid surface, e.g. roughness, and the type of fluid.

Table 2 below gives the results of calculation of fractional volume occupied by pores of different diameters from PPT. Similar calculations are made for MIP but are not shown here. The typical parameters adopted for nitrogen and mercury for interpretation of PPT and MIP tests, respectively, are listed at the bottom of the Table 2.

Since nitrogen is not allowed to escape from the ceramic disc due to its high entry value, the outflow of water represents the volume of the pore of certain size. Thus a cumulative pore volume versus pore diameter curve of PPT can be obtained and is shown in Fig. 5.

Next we compare the results of POSD from PPT with that obtained from MIP. The POSD of porous media can be characterised by either cumulative pore volume-diameter graphs or pore diameter density function curves. Cumulative pore volume-diameter graphs obtained from PPT & MIP for the same soil are shown in Fig. 5. It is noted that the two results are in reasonable agreement thereby proving that PPT can be used to obtain cumulative pore volume and pore-size relationship. The pore diameters in PPT cover a range from about 200 nm to 280 μm. On the other hand, the pore diameters in MIP test cover a much wider range i.e. from about 10 nm to 280 μm but data for this range are not shown on the graph. A coefficient of correlation between PPT & MIP results is 0.949.

The pore diameter density function curve can be computed from the cumulative curve. If the range of pore-diameters is subdivided into a number of parts, and the corresponding pore volumes are plotted as ordinates, a histogram of pore diameters is obtained. The pore diameter density function curve is simply obtained by plotting the pore-diameters against the slope of the cumulative pore volume curve in Fig. 5. Computation of slope of cumulative pore volume curve is a process of numerical differentiation which can lead to inaccuracies. Fig. 6 shows the pore diameter density function curves obtained from PPT as well as from MIP. Here only the range of diameters penetrated under a suction pressure up to a maximum of 1200 kPa are considered. The two results match well except for few points corresponding to very small pore size.

From our results of PPT, it can be found that the SWRC obtained from PPT can be used for predicting POSD of soils. In order to better validate the method of deducing POSD from SWRC, other experimental results of SWRCs measured by PPT and Vapour equilibrium readings are used in this study and the calculated cumulative pore volume-diameter curves are given in Figs. 7&8. Fig. 7 a&b show the pore structures of colluvial soils (Zhang and Li, 2010) with 40% (ML) and 58% (SC) coarse contents, respectively. Fig. 7c gives the pore structures of Opalinus clay (Romero and Simms, 2008). It can be found that the cumulative pore volume-diameter curves obtained from MIP and PPT of soil ML and Opalinus clay agree very well. While the pore structures of soil SC is not so good. In Fig. 8, the pore structures of soft clay (Romero and Simms, 2008) deduced from SWRC are compared to MIP data and a good agreement can be observed. Hence, it can be reached that there lies a better correlation between POSD and SWRC, and the determination of POSD from SWRC is reliable for most of soils and rocks.

It should be noticed that both measurements of SWRC and POSD are not easy. MIP is simpler compared to PPT, it can be finished within a couple of hours; whilst it is not a part of standard soil mechanics laboratory equipment and the MIP test is expensive. The testing process of PPT is time-consuming, especially for clayey and fine grained soils. Besides, the determination of POSD from PPT may be only valid for SWRC during a drying process and the curve obtained from PPT is only part of the whole one due to the limited gas pressure. However, from the correlation between SWRC and POSD, we can use the SWRC, a compete one, measured by other simple techniques, e.g. tensiometers, contact filter paper techniques, to predict POSD curves. Although MIP has been widely accepted in the determination of POSD of soils, some researchers argue the high pressure may cause volume change. However, this effect can be neglected in PPT as the pressure is much lower than that in MIP.

Conclusions

In this paper, a comparison of pore-size distribution of a soil obtained by two different methods is made based on certain assumptions discussed. The following conclusions can be drawn. The PPT is a type of gas intrusion test and it can be used for obtaining pore size distribution of a soil in the same manner as MIP. The cumulative pore size distribution curve and pore size density function curve match well with those obtained from MIP within the range of pore sizes governed by suction pressures used. This research indicates that the SWRC, obtained from other techniques such as those which use a tensiometer or a contact filter paper may yield pore-size distribution over a much larger range of pores, thus confirming the validity of assumptions made.

References

Arya, L. M., Leij, F. J., Shouse, P. J. & Van Genuchten, M. T. 1999. Relationship between the Hydraulic Conductivity Function and the Particle-Size Distribution. *Soil Sci. Soc. Am. J.,* 63**,** 1063-1070.

Arya, L. M. & Paris, J. F. 1981. A Physicoempirical Model to Predict the Soil Moisture Characteristic from Particle-Size Distribution and Bulk Density Data. *Soil Sci. Soc. Am. J.,* 45**,** 1023-1030.

Bryant, S. & Blunt, M. 1992. Prediction of relative permeability in simple porous media. *Physical Review A,* 46**,** 2004-2011.

Delage, P. 2007. Microstructure Features in the Behaviour of Engineered Barriers for Nuclear Waste Disposal. *In:* SCHANZ, T. (ed.) *Experimental Unsaturated Soil Mechanics.* Springer Berlin Heidelberg.

Diamond, S. 1970. Pore size distributions in clays. *Clays and Clay Minerals,* 18**,** 7-23.

Doktor, T., Kytyr, D., Valach, J. & Jirousek, O. Assessment of pore size distribution using image analysis. Youth Symposium on Experimental Solid Mechanics, 2010.

Drake, L. C. 1949. Pore-Size Distribution in Porous Materials. *Industrial & Engineering Chemistry,* 41**,** 780-785.

Dullien, F. a. L. 1991. *Porous Media, Second Edition: Fluid Transport and Pore Structure*, Academic Press.

Echeverría, J. C., Morera, M. T., Mazkiarán, C. & Garrido, J. J. 1999. Characterization of the porous structure of soils: adsorption of nitrogen (77 K) and carbon dioxide (273 K), and mercury porosimetry. *European Journal of Soil Science,* 50**,** 497-503.

Gibson, L. J. & Ashby, M. F. 1999. *Cellular Solids: Structure and Properties*, Cambridge University Press.

Imre, E., Rajkai, K., Firgi, T., Laufer, I., Genovese, R. & Jommi, C. 2012. Modified Grading Curve – SWCC Relations. *In:* MANCUSO, C., JOMMI, C. & D'ONZA, F. (eds.) *Unsaturated Soils: Research and Applications.* Springer Berlin Heidelberg.

Kuila, U. & Prasad, M. 2013. Specific surface area and pore-size distribution in clays and shales. *Geophysical Prospecting,* 61**,** 341-362.

Lindquist, W. B., Venkatarangan, A., Dunsmuir, J. & Wong, T.-F. 2000. Pore and throat size distributions measured from synchrotron X-ray tomographic images of Fontainebleau sandstones. *Journal of Geophysical Research: Solid Earth,* 105**,** 21509-21527.

Penumadu, D. & Dean, J. 2000. Compressibility effect in evaluating the pore-size distribution of kaolin clay using mercury intrusion porosimetry. *Canadian Geotechnical Journal,* 37**,** 393-405.

Pietruszczak, S. & Pande, G. 1996. Constitutive Relations for Partially Saturated Soils Containing Gas Inclusions. *Journal of Geotechnical Engineering,* 122**,** 50-59.

Pietruszczak, S. & Pande, G. N. 1991. On the mechanics of partially saturated soils. *Computers and*

Geotechnics, 12**,** 55-71.

Prapaharan, S., Altschaeffl, A. & Dempsey, B. 1985. Moisture Curve of Compacted Clay: Mercury Intrusion Method. *Journal of Geotechnical Engineering,* 111**,** 1139-1143.

Richards, L. A. 1941. A pressure-membrane extraction apparatus for soil solution. *Soil Science,* 51**,** 377-386.

Romero, E. & Simms, P. H. 2008. Microstructure Investigation in Unsaturated Soils: A Review with Special Attention to Contribution of Mercury Intrusion Porosimetry and Environmental Scanning Electron Microscopy. *Geotechnical and Geological Engineering,* 26**,** 705-727.

Shin, H. S., Kim, K. Y. & Pande, G. N. 2013. Porosity and Pore-Size Distribution of Geomaterials from X-ray CT Scans. *In:* LALOUI, L. & FERRARI, A. (eds.) *Multiphysical Testing of Soils and Shales.* Springer Berlin Heidelberg.

Shin, H. S., Kim, K. Y. & Pande, G. N. 2015. On computation of strain-dependent permeability of rocks and rock-like porous media. *International Journal for Numerical and Analytical Methods in Geomechanics,* 39**,** 821- 832.

Simms, P. & Yanful, E. 2002. Predicting soil-water characteristic curves of compacted plastic soils from measured pore-size distributions. *Geotechnique,* 52**,** 269-278.

Wang, M., Kong, L. & Zang, M. 2015. Effects of sample dimensions and shapes on measuring soil–water characteristic curves using pressure plate. *Journal of Rock Mechanics and Geotechnical Engineering,* http://dx.doi.org/10.1016/j.jrmge.2015.01.002.

Zhang, L. M. & Li, X. 2010. Microporosity Structure of Coarse Granular Soils. *Journal of Geotechnical and Geoenvironmental Engineering,* 136**,** 1425-1436.

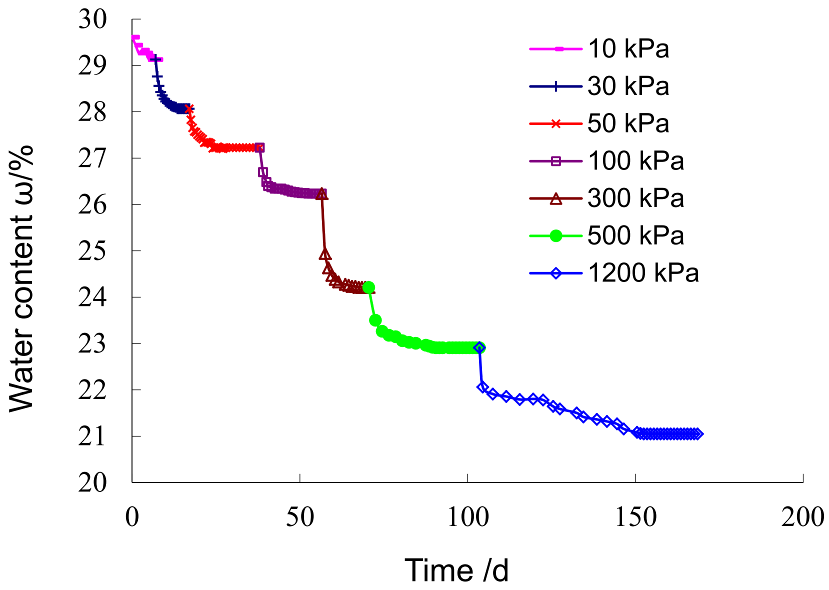

Water content ω/%
Time /d
10 kPa
30 kPa
50 kPa
100 kPa
300 kPa
500 kPa
1200 kPa

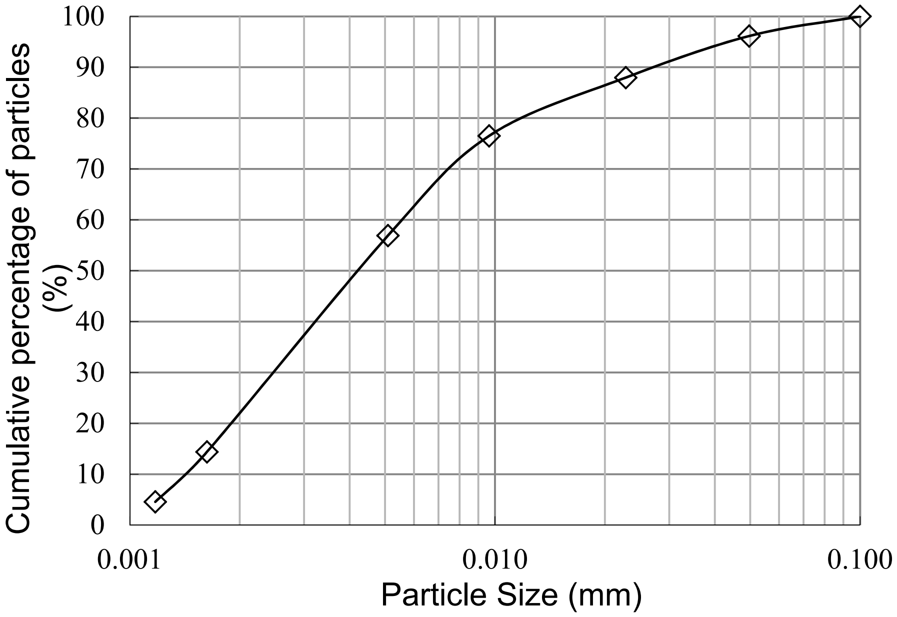

Cumulative percentage of particles (%)
100
90
80
70
60
50
40
30
20
10
0
0.001
0.010
0.100
Particle Size (mm)

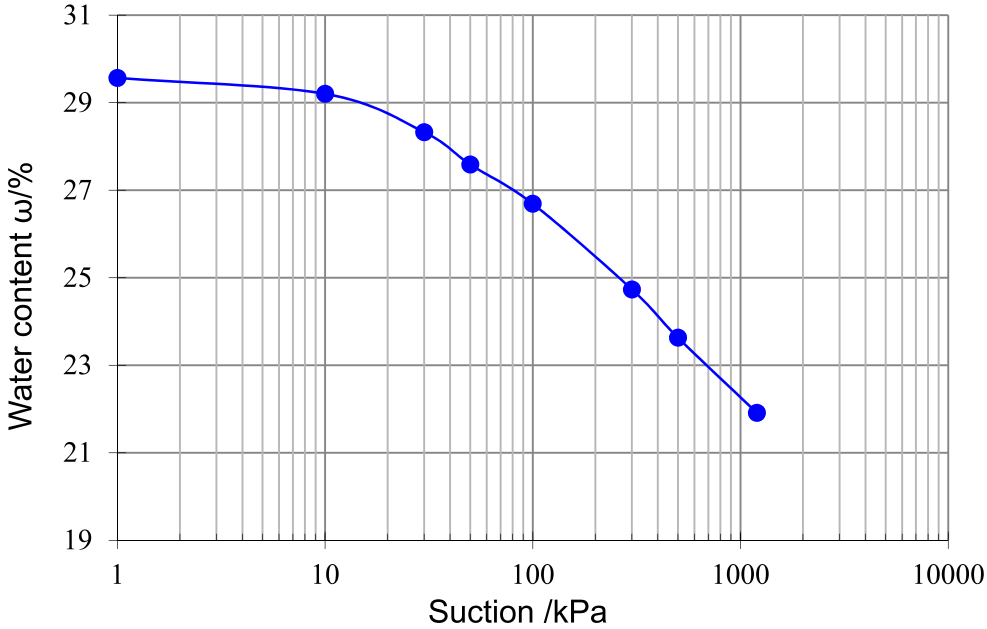

31
29
27
25
23
21
19
Water content ω/%
1
10
100
1000
10000
Suction /kPa

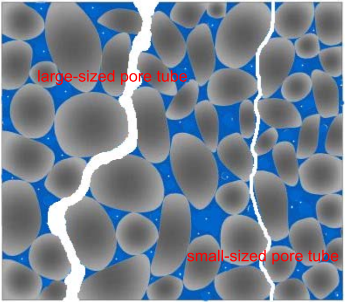
large-sized pore tube
small-sized pore tube

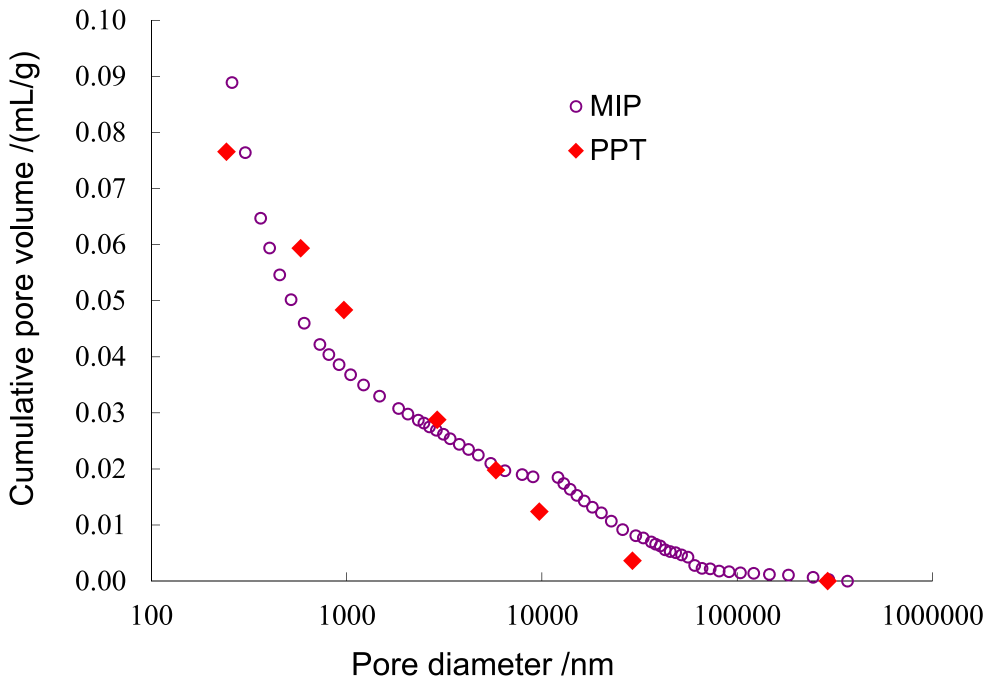

Cumulative pore volume /(mL/g)
0.10
0.09
0.08
0.07
0.06
0.05
0.04
0.03
0.02
0.01
0.00
MIP
PPT
100
1000
10000
100000
1000000
Pore diameter /nm

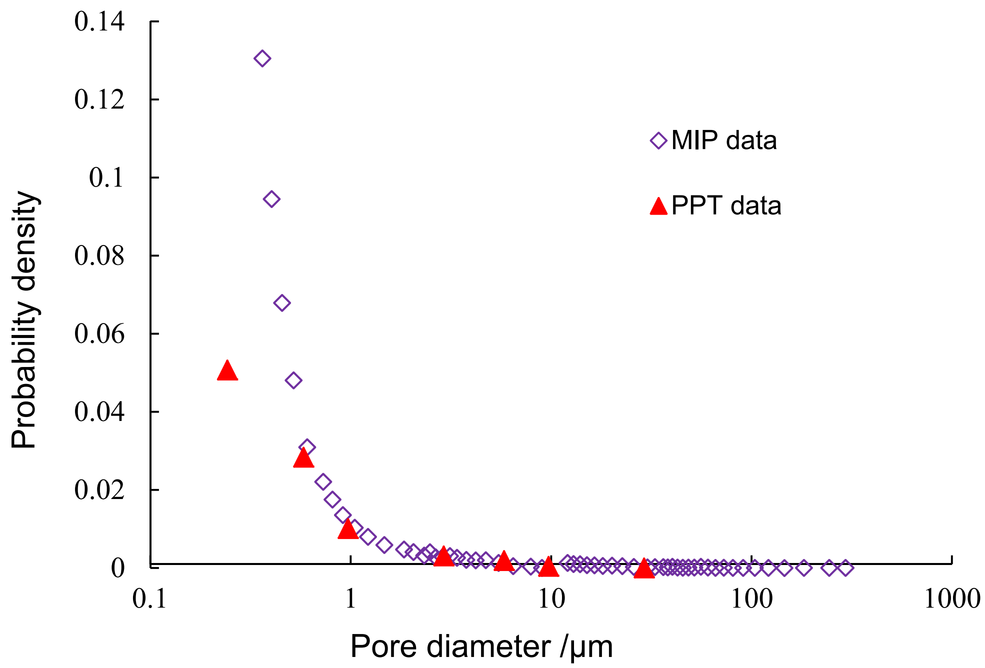

0.14
0.12
0.1
0.08
0.06
0.04
0.02
0
Probability density
MIP data
PPT data
0.1
1
10
100
1000
Pore diameter /μm

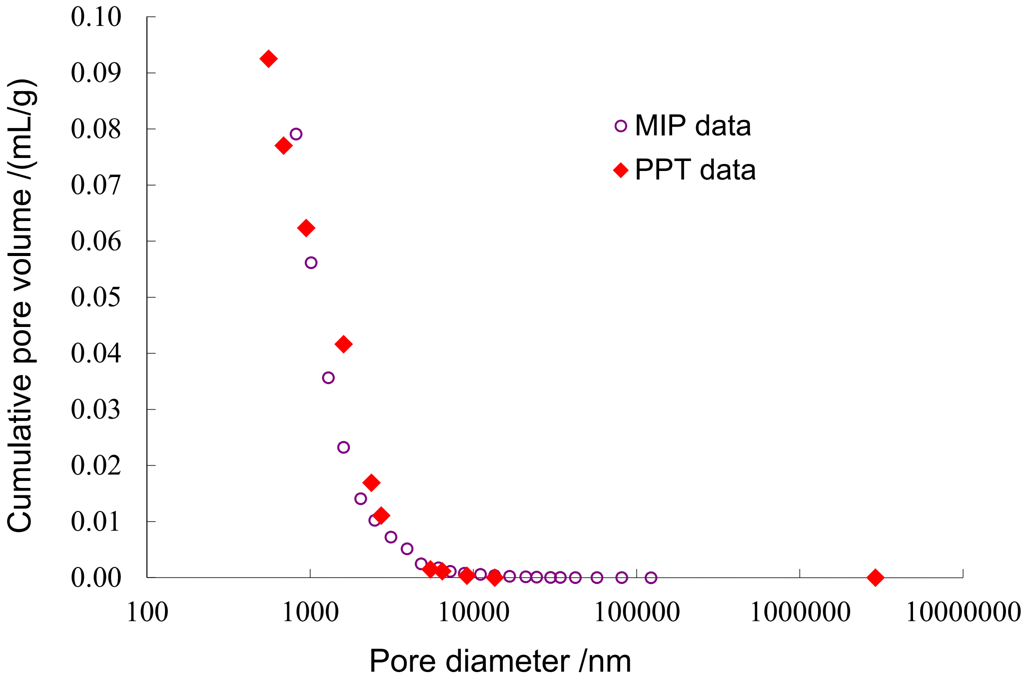
0.10
0.09
0.08
0.07
0.06
0.05
0.04
0.03
0.02
0.01
0.00
Cumulative pore volume /(mL/g)
MIP data
PPT data
100
1000
10000
100000
1000000
10000000
Pore diameter /nm

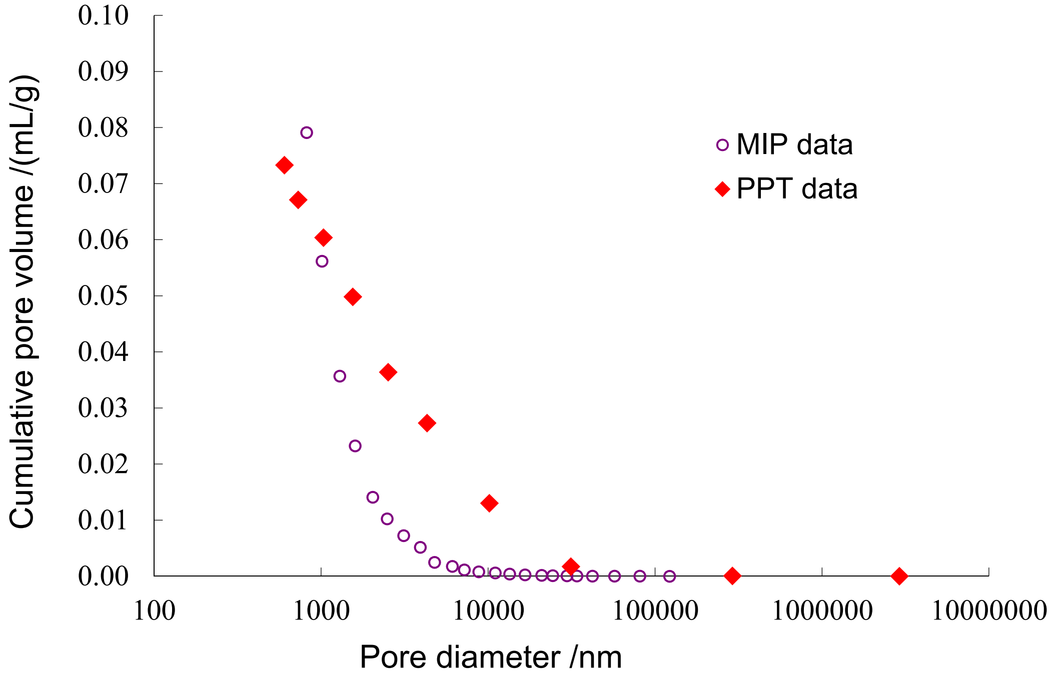

Cumulative pore volume /(mL/g)
0.10
0.09
0.08
0.07
0.06
0.05
0.04
0.03
0.02
0.01
0.00
100
1000
10000
100000
1000000
10000000
Pore diameter /nm
MIP data
PPT data

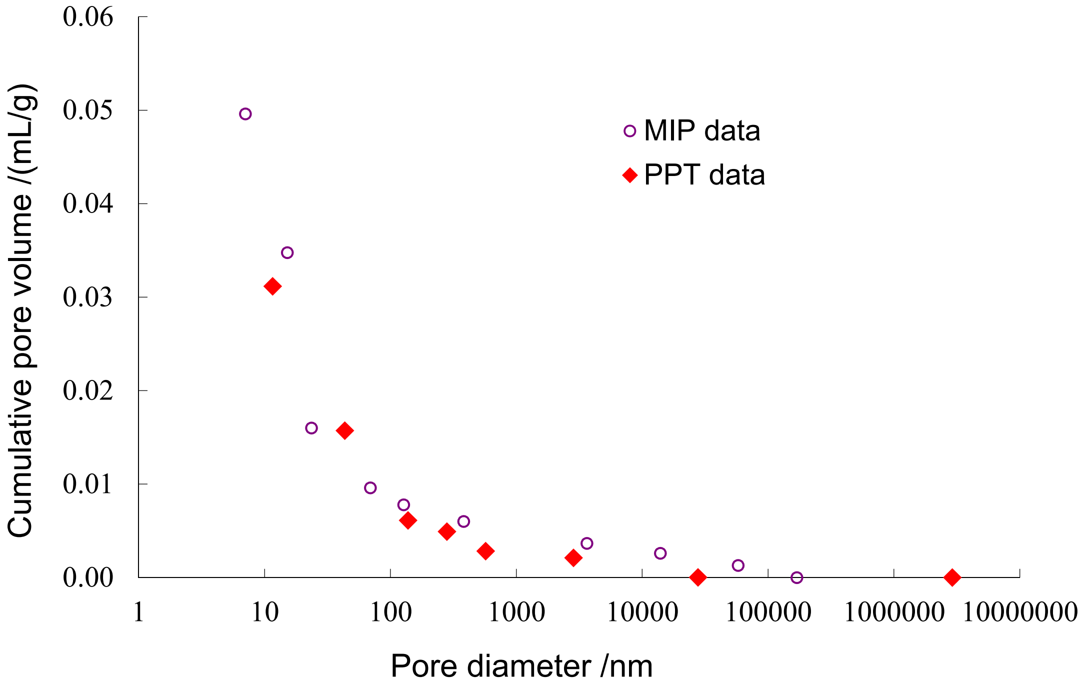

0.06
0.05
0.04
0.03
0.02
0.01
0.00
Cumulative pore volume /(mL/g)
MIP data
PPT data
1
10
100
1000
10000
100000
1000000
10000000
Pore diameter /nm

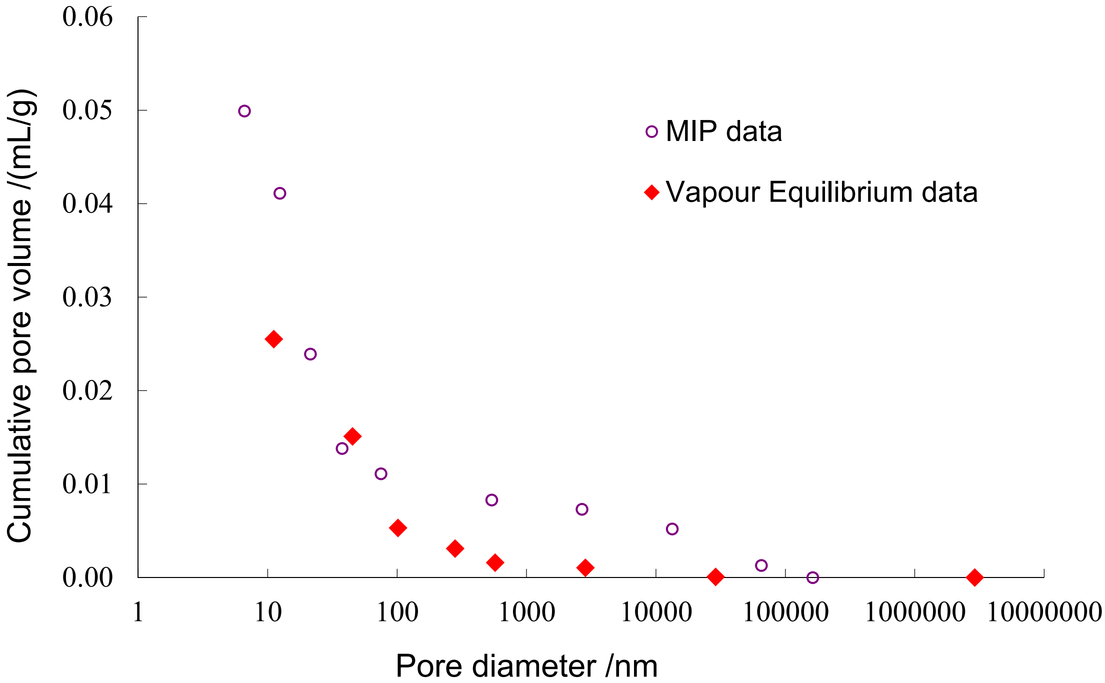

Cumulative pore volume /(mL/g)
0.06
0.05
0.04
0.03
0.02
0.01
0.00
MIP data
Vapour Equilibrium data
1
10
100
1000
10000
100000
1000000
10000000
Pore diameter /nm

Table 1 Basic physical properties of expansive soil

Density/g/cm^3	Natural Water Content/％	Dry Density/g/cm^3	Specific Gravity	Liquid Limit/％	Plastic Limit/％	Plasticity Index	Clay Content(<2μm)/％
1.95	27.0	1.53	2.74	68.9	28.2	40.7	37.0

Table 2 Calculation of fractional volume from PPT

Suction (kPa)	Water Content (%)	Pore diameter (nm)	Accumulative pore volume(ml/g)	Fractional volume (%)
1	29.566	291000	0	0
10	29.202	29100	0.003635703	1.229523017
30	28.325	9700	0.012404	2.96532
50	27.588	5852	0.019782	2.495208
100	26.689	2910	0.0287648	3.0376451
300	24.733	970	0.04833346	6.61772683
500	23.631	582	0.0593475	3.72473149
1200	21.910	242.5	0.076563619	5.822153112

(for Mercury Intrusion surface tension *Ts* =0.480 N/m and contact angle α = 140°; while for Gas Intrusion Surface tension is 0.07275 N/m and the contact angle is 180°)